Fracture behavior of nitrile rubber-cellulose II nanocomposites

Vera Lucia C. Lapa · João Carlos Miguez Suarez ·
Leila Lea Y. Visconte · Regina Célia Reis Nunes

Abstract Nanocomposites of nitrile rubber (NBR) and cellulose II (Cel II) were prepared by co-coagulation of nitrile rubber latex and cellulose xanthate mixtures. The effect of the addition of increasing amounts of Cell II, varying from 0 to 30 phr, on the mechanical behavior of a NBR was analyzed. The fracture mechanisms of the nitrile rubber-cellulose II (NBR/Cel II) nanocomposites after tension and tear tests was investigated by scanning electron microscopy (SEM) and correlated to the test results. It was found that the addition of Cell II to NBR leads to a gradual change in the stress at break, and the samples with 20 phr of Cel II showed the highest resistance; as the cellulose content is increased to 30 phr, the strain at break decreases. The SEM fractographic analyses of NBR/Cel II nanocomposites, with cellulose content up to 30 support the observed mechanical behavior of the material. The results are presented and discussed. The obtainment of NBR/Cel II nanocomposites was proven by transmission electron microscopy (TEM).

Introduction

The addition of fillers into elastomers has technological significance due to the enhancement of several engineering

V. L. C. Lapa · L. L. Y. Visconte · R. C. R. Nunes (✉)
Instituto de Macromoléculas Professora Eloísa Mano,
Universidade Federal do Rio de Janeiro, P.O. Box 68525, Rio de
Janeiro 21945-970 RJ, Brazil
e-mail: rcnunes@ima.ufrj.br

J. C. Miguez Suarez
Instituto Militar de Engenharia, Seção de Engenharia
Mecânica e de Materiais, Praça General Tibúrcio, 80,
Rio de Janeiro 22290-270 RJ, Brazil
e-mail: jmiguez@ime.eb.br

characteristics and the cheapening of the compound. The improvement of certain characteristics, particularly the mechanical properties (strength, wear resistance, energy loss, resilience, etc.), is normally achieved by the addition of several materials, especially carbon black and silica. The filler potential reinforcement capability depend on its own characteristics, as well as on its interaction with the matrix and dispersion [1–3].

It has been shown that incorporation of cellulose II (Cell II) to a rubber matrix produces composites with adequate properties [4–7]. The reinforcement has normally been expressed by enhancement in modulus and mechanical properties of the vulcanizates. Rubber compounds, when applied in engineering components, must rely on their high performance which depend of failure properties and service conditions. In the special case of cellulose acting as filler, the reinforcing efficiency is related to the nature of cellulose itself, in particular the degree of cristallinity, which in turn is dictated by the molecular weight. In consequence, the resulting morphological structure plays an important role in the improvement of the mechanical behavior of rubber composites and a better understanding of the failure modes is important to predict the service life of these materials [7–10]. The use of Cell II as reinforcement for natural and synthetic rubbers and the nanocomposite formation by co-coagulation system were described in previous works [11–14].

Scanning electron microscopy is an important tool to determine fracture patterns and the mechanical behavior of polymers that can be interpreted in terms of the microscopical failure mechanisms [10, 15].

The aim of the present work was to investigate the influence of increasing amounts of Cell II addition on the fracture behavior of nitrile rubber (NBR) nanocomposites. Through transmission electron microscopy (TEM) these

composites were found to contain Cel II dispersed at the nanoscale range.

Experimental

Coprecipitation process

The coprecipitation of nitrile rubber latex with cellulose xanthate was performed by adding, under stirring, nitrile rubber latex/cellulose xanthate mixture to an equimolar acid solution of sulfuric acid and zinc sulfate. This process is efficient for the regeneration of cellulose xanthate because the initial orange color becomes white after acid solution addition. The cellulose xanthate volume was calculated as to have 10, 20 and 30 phr of Cell II in the final product. For process control, the viscosity of the system was maintained constant in all compositions by keeping the same xanthate/water ratio. During the decomposition of cellulose xanthate, production of CS_2, H_2S and CO_2 gases takes place. After coagulation, the fine rubber-cellulose particles were washed with distilled water to remove residual acidity. The product was separated from the aqueous suspension by filtration and then dried in an air-circulating oven at 50 °C [13, 16].

The characteristics of the products used were:

- NBR—33% acrylonitrile content, 56 Mooney viscosity [ML (1 + 4) @100] and 25% total solids, supplied by NITRIFLEX S.A. Indústria e Comércio, Rio de Janeiro, Brazil.
- Alkali-soluble cellulose xanthate—8% cellulose, 2.1% total sulfur, 4.9% NaOH, 6.43% salt index, from VICUNHA Têxtil S.A., São Paulo, Brazil.
- Sulfuric acid P.A., VETEC, Rio de Janeiro, Brazil.
- Zinc sulfate P.A., VETEC, Rio de Janeiro, Brazil.

NBR-cellulose II compounds and determination of cure parameters and vulcanization

Vulcanizable NBR-Cel II compositions were prepared in a Berstorff two-roll mill at 50 °C according to the following formulation (ASTM D 3187), in phr (parts per hundred resin): 100 NBR; 3.0 zinc oxide; 1.5 sulfur; 1.0 stearic acid; 0.7 N-tert-butyl-2-benzothiazolesulfenamida (TBBS). The cure parameters were determined according to ASTM D 2084 on an Oscillating Disk Rheometer model 100 S from Monsanto, operating at 150 °C and 1° arc. The vulcanization at optimum cure times was carried out at 150 °C and 3 MPa in an electrically heated hydraulic press. From the resulting vulcanized sheets, samples for the mechanical tests were cut.

Mechanical tests

The tension and tear tests were performed in a model 1101 INSTRON Universal Testing Machine at a crosshead speed of 500 mm/min at room temperature using specimens punched out from the molded vulcanized sheets. Tensile testing followed ASTM D 412, using dumb-bell specimens. The tear strength was measured on unnotched 90° angle test specimen according to ASTM D 624. The median value measured over five specimens was taken as the test result for each compound tested.

Fractographic analyses

After tension and tear tests both specimens fragments were collected for microscopic examination in a model JSM 5800LV JEOL scanning electron microscope (SEM). Fractographic analyses were carried out by direct observation of the topography of fracture surfaces of tensile and tear specimens after being sputter coated with gold in a vacuum chamber.

Morphological analyses

The phase morphology was examined on a Transmission Electron Microscopy Hitachi H-800MT using thin samples (maximum, 100 nm thick) prepared in an ultramicrotome at cryogenic temperatures.

Results and discussion

Mechanical properties

Results of mechanical properties as stress at break, strain at break, modulus at 100% and tear resistance are presented in Table 1. When compared with pure gum (composition without filler), it is possible to see that the nanocomposites presented some differences in the mechanical properties.

The addition of Cell II to NBR leads to a gradual change in the stress at break, and the amount of 20 phr imparted the highest stress, thus, indicating that there is an upper limit for cellulose amount in order to achieve the maximum property. As Cell II content is further increased to 30 phr, the elongation at break decreases while the tear strength and modulus results show a continuous enhancement. The results permit to confirm the reinforcing character of Cell II, when present in a NBR matrix as the stress at break and modulus at 100% for 20 phr of Cel II composition show increases of 70 and 100%, respectively, compared to pure rubber. Typical stress–strain curves are presented in Fig. 1 to corroborate these results.

Table 1 Mechanical properties of NBR/Cel II nanocomposites

| NBR/Cel II	Stress at break (MPa)	Strain at break (%)	Modulus at 100% (MPa)	Tear strength (kN/m)
100/0	3.4 ± 0.76	600 ± 26.5	1.07 ± 0.67	15.24 ± 1.08
100/10	6.1 ± 0.48	675 ± 25.0	1.30 ± 0.73	19.55 ± 2.83
100/20	6.8 ± 0.79	700 ± 50.0	1.73 ± 0.89	24.37 ± 3.06
100/30	5.5 ± 0.61	450 ± 28.9	2.78 ± 0.59	27.48 ± 2.46
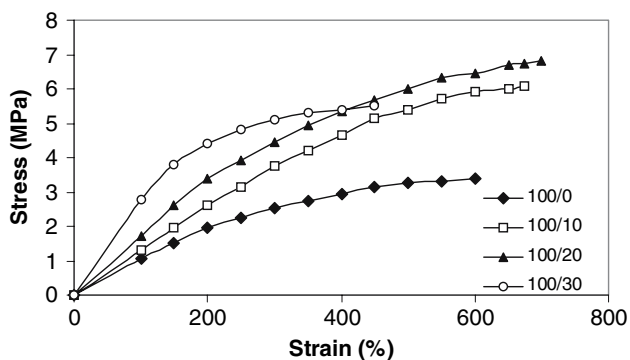
Fig. 1 Stress × strain of NBR/Cel II nanocomposites

Scanning electron microscopy

Typical SEM photomicrographs of the fracture surfaces of the specimens submitted to tension and tear tests are presented in Figs. 2–5. These vulcanized nitrile rubber composites without and with Cell II addition show characteristic features of fracture mechanisms for composite materials. The images show that Cell II addition to NBR matrix considerably modifies the rubber fracture mechanisms, both in tension and in tear. The different topographic aspects indicate that the mechanical behavior of the nitrile rubber is modified in the presence of Cell II.

Scanning electron microscopy in tension samples

After the tensile tests, it was observed that all tension specimens showed normal fracture and that the 10 and 20 phr samples exhibited a whitening phenomenon in the
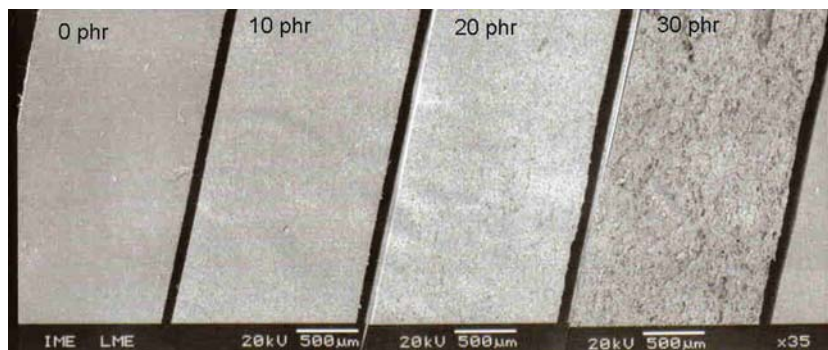
fracture region, as an indicative of plasticity in these compositions. Normal fracture, or normal rupture, is a type of fracture where the crack grows in a direction perpendicular to the loading axis until it approaches the surface of the specimen and the fracture plane is nearly normal to the applied stress. This fracture mode occurs principally under the influence of uniform plastic strain in the direction of the applied stress [10, 17]

Figures 2 and 3 show SEM photomicrographs of the failure surfaces of NBR/Cel II tension specimens tested showing modifications in the fracture mechanisms.

At low magnification, as in Fig. 2, it can be seen that the fracture topography changes, upon Cel II addition, from a smooth, flat surface, developed by a typical fracture mechanism for elastomers, observed in the unfilled rubber (0 phr), into a rough, irregular surface presented by the filled compositions. The roughness increases as Cell II content also increases, showing that the addition of high Cell II contents induces plastic deformation and a fracture mechanism transition.

At higher magnification the changes in the topography of fracture surfaces are clearly identified (Fig. 3). The addition of a small amount of Cel II (10 phr) to the NBR matrix did not impart great modifications in the rubber basic tensile fracture mechanisms, when compared with the unfilled material (Fig. 3a), the 10 phr Cell II sample presents a small increase in roughness showing relatively smooth fracture surface and slight ridges (Fig. 3b) and loss of the characteristic rubbery aspect. Increasing the Cell II content from 10 to 20 phr, a few alterations are detected with the appearance of plain facets and small particles, firmly attached to the matrix (Fig. 3c). These fractographic aspects indicate that the

Fig. 2 Scanning electron microscopy photomicrographs, at low magnification, of tension fracture surfaces of NBR/Cel II nanocomposites

Fig. 3 Scanning electron microscopy photomicrographs, at higher magnification, of tension fracture surfaces of NBR/Cel II nanocomposites: (**a**) 0 phr; (**b**) 10 phr; (**c**) 20 phr; (**d**) 30 phr
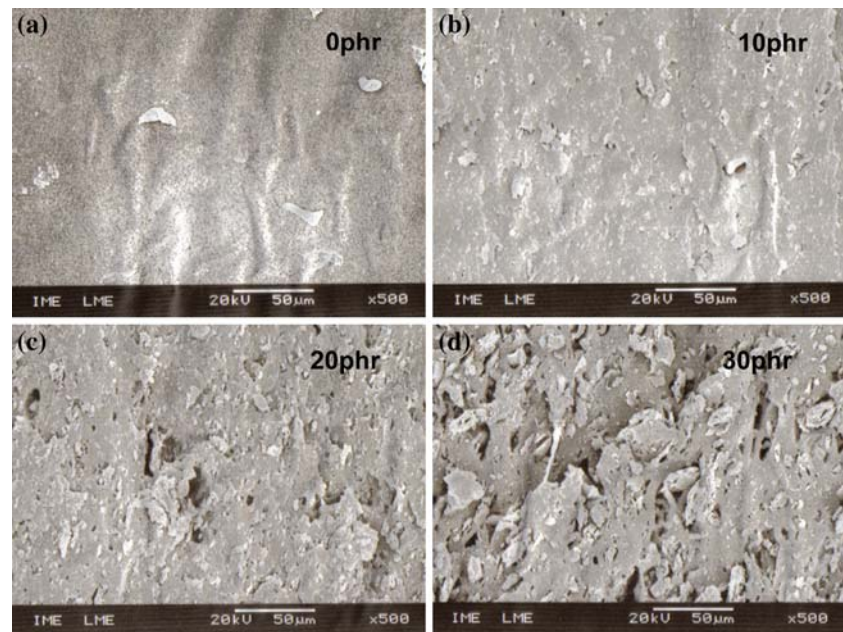
10 and 20 phr compositions present a homogeneous fracture behavior and that, for these concentrations, there is a good compatibility between NBR and Cell II leading to an effective interaction matrix-filler and indicating an enhancement on the mechanical properties. Physical interactions can be responsible for the compatibility. Further increase of Cell II content to 30 phr remarkably changes the fracture topography; the fracture surfaces become highly rough, with a large number of particles coming out of the matrix fracture plane, which characterizes a fracture mechanism, similar to the fiber pull-out phenomenon and suggesting the occurrence of a weak interaction matrix-filler at this level of Cel II content and possibility the occurrence of crack deflection process (Fig. 3d). The agglomerates that come out of the matrix provide an easy path for crack propagation, thus reducing the ductility of the material, as indicated by a decrease in the elongation at break of the 30 phr NBR/Cel II nanocomposites.
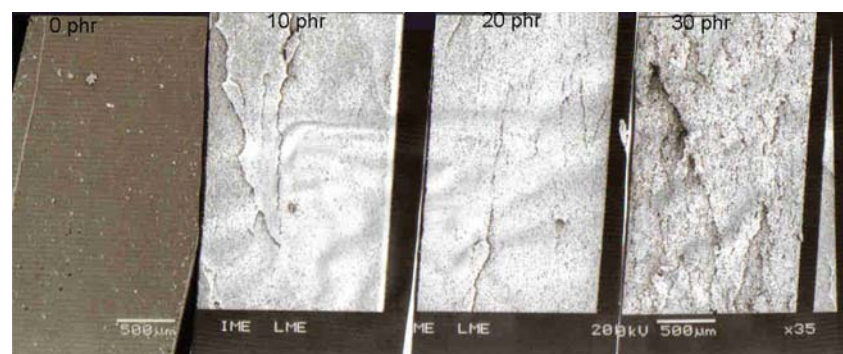
Scanning electron microscopy in tear samples

Typical SEM photomicrographs of the fracture surfaces of tear test specimens are shown in Figs. 4 and 5. The tear resistance of NBR-Cell II samples can be correlated to the roughness of the fracture surfaces and to the existence of random agglomerates.

Figure 4 shows, at low magnification, the SEM topographical features of the tear fracture surfaces. As Cell II content increases there is a drastic modification in the topography of the fracture surfaces that changes from a relatively smooth aspect, in the unfilled NBR, to a highly rough one in the 30 phr Cell II material.

The fractographic observation at a higher magnification (Fig. 5) permits an adequate analysis of the fracture behavior. The unfilled material shows flat surface with a main slip line, a characteristic aspect of the tear fracture of rubber vulcanizates (Fig. 5a). The addition of 10 and 20 phr of Cell II to NBR causes small changes in the

Fig. 4 Scanning electron microscopy photomicrographs, at low magnification, of tear fracture surfaces of NBR/Cel II nanocomposites

Fig. 5 Scanning electron microscopy photomicrographs, at higher magnification, of tear fracture surfaces of NBR/Cel II nanocomposites: (**a**) 0 phr; (**b**) 10 phr; (**c**) 20 phr; (**d**) 30 phr
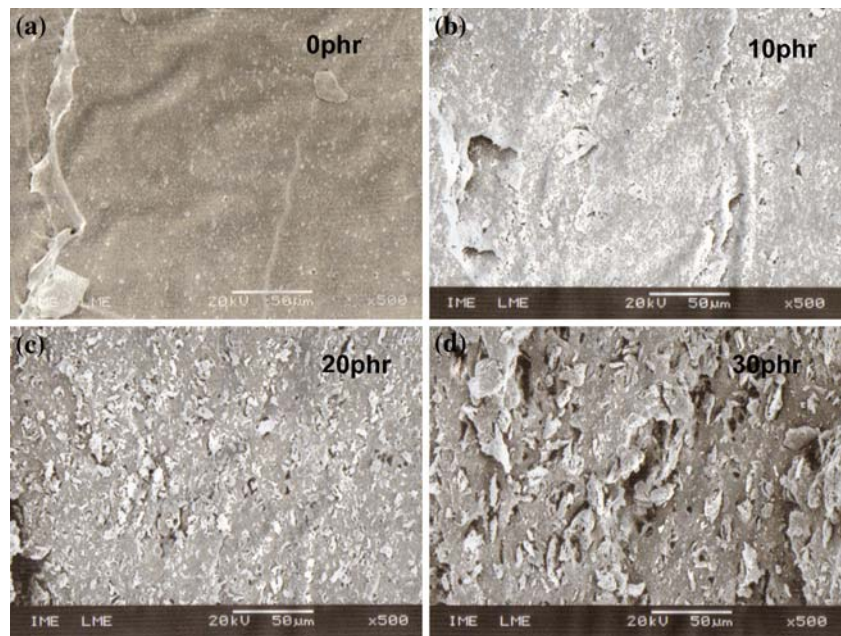

topographic aspect; the fracture surfaces are no longer totally planar and coarser slip lines (Fig. 5b–c) start to show up, an indicative that at these Cell II levels, a good interaction matrix- Cell II is achieved, as already observed for the tensile samples. The occurrence of these slip lines also shows that the fracture propagation process occurs with a high energy dissipation suggesting that the nanocomposites with these Cell II contents should have good tear strength. The 30 phr Cell II samples present a rough surface with random agglomerates distributed in the matrix

plan, voids and wrinkles, which indicate a modification in the fracture mode (Fig. 5d). These topographical features show that the propagation of the fracture in the rubber matrix is discontinuous so that the 30 phr nanocomposites should offer a good resistance to tearing.

The SEM fractographic analysis is in agreement with the mechanical test results and supports the observed changes in the NBR/Cel II nanocomposites properties as the Cel II content increases.

Transmission electron microscopy

The nanocomposite character of this NBR/Cel II system was proven by TEM. Figure 6 presents a TEM photomicrography of a NBR/Cel II sample containing 20 phr of Cel II where it is possible to verify that the Cel II particles (dark regions) have nanometric dimensions. Cell II is well dispersed although the dimensions are not uniform.
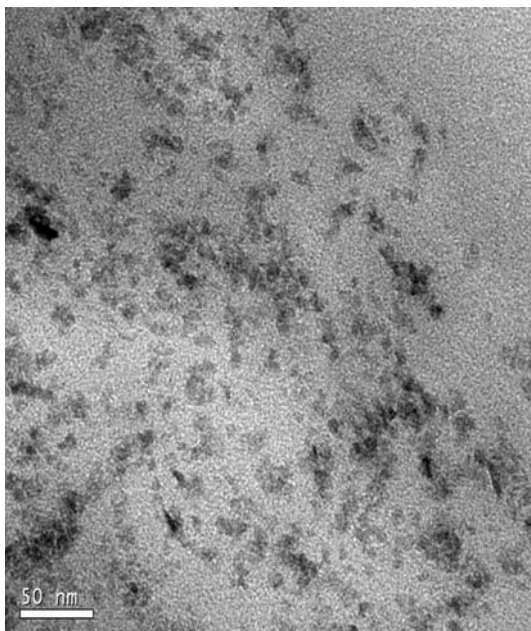
Fig. 6 Transmission Electron Microscopy photomicrography of NBR/Cel II nanocomposite containing 20 phr of Cel II

Conclusions

– The system used to incorporate cellulose into NBR promoted the formation of a nanocomposite material. This results was supported by TEM.
– Cellulose II was found to have large influence on mechanical properties of the nitrile rubber compositions studied. The upper limit of Cell II content for a positive effect is 20 phr.
– The Scanning Electron Microscopy features of NBR/Cel II nanocomposites, in the filler range investigated are in agreement with the mechanical tests results and

support the observed mechanical behavior of the nanocomposites.

References

1. Arroyo M, López-Manchado MA, Herrero B (2003) Polymer 44:2447
2. Boonstra BB (1979) Polymer 20:691
3. Shadu S, Bhowmick AK (2005) J Mater Sci 49:1663
4. Nunes RCR, Mano EB (1995) Polym Compos 16(5):241
5. Vieira A, Nunes RCR, Costa DMR (1997) Polym Bull 39:117
6. Affonso JES, Nunes RCR (1995) Polym Bull 34:669
7. Nunes RCR, Visconte LLY (2000) Natural fibers reinforced elastomeric composites. In: Frollini E, Leão AL, Mattoso LHC (eds) Natural polymers and agrofibers composites. Embrapa Instrumentação Agropecuária, SP, Brazil, 135
8. Allen SL, Turvey RW, Bolker HI (1975) Appl Polym Sympos 3(28):903
9. Zugenmaier P (2001) Prog Polym Sci 26:1341
10. Martins AF, Miguez Suarez JC, Visconte LLY, Nunes RCR (2003) J Mater Sci 38:2415
11. Martins AF, Visconte LLY, Schuster RH, Boller F, Nunes RCR (2004) Kautsch Gummi Kunstst 57(9):446
12. Martins AF (2002) PhD Thesis, Instituto de Macromoléculas Professora Eloisa Mano, Universidade Federal do Rio de Janeiro, Brazil
13. Peres ECC, Nunes RCR, Visconte LLY (2001) *PI 0105116-4*
14. Brandt K, Schuster RH, Nunes RCR (2006) Kautsch Gummi Kunstst 59(10):511
15. Agarwal K, Setua DK, Sekhar K (2005) Polym Test 24(6):781
16. Nunes RCR, Martins AF, Visconte LLY, Pereira RA, Perez CAC, Mano EB (2004) J Rubber Res 7(1):1
17. Chawla KK (1998) Composite materials—science and engineering, 2nd edn. Springer-Verlag, New York